RSC Advances

PAPER

View Article Online
View Journal | View Issue

Cite this: *RSC Adv.*, 2017, **7**, 41862

Magnetic solid phase extraction with octahedral structured Fe_3O_4@SiO_2@polydimethylsiloxane magnetic nanoparticles as the sorbent for determining benzene, toluene, ethylbenzene and xylenes in water samples

Maosheng Zhang, *[a] Guobin Huang,[a] Jiarong Huang,[b] Ling Zhong[a] and Weilan Chen[a]

Novel octahedral structured Fe_3O_4@SiO_2@polydimethylsiloxane magnetic nanoparticles (Fe_3O_4@SiO_2@PDMS MNPs) have been successfully synthesized for the first time. The magnetic nanoparticles (MNPs) were characterized by scanning electron microscopy, transmission electron microscopy, X-ray diffraction, Fourier transform infrared spectrometry and vibrating sample magnetometry. The Fe_3O_4@SiO_2@PDMS MNPs were used as the sorbent for magnetic solid phase extraction (MSPE) to determine benzene, toluene, ethylbenzene and xylenes (BTEX) in water samples. Extraction parameters, the amount of sorbent, the extraction time, the stirring rate, the salt effect, the type of desorption solvent, the volume of desorption solvent and the desorption time were optimized. The optimal extraction conditions were amount of sorbent, 100 mg; extraction time, 15 min; stirring rate, 200 rpm; no salt; desorption solvent, dichloromethane; volume of desorption solvent, 0.5 mL; and desorption time, 1.0 min. Good linearity was observed in the calibration range from 0.05 to 20 μg L^{-1}, and the coefficient of determination (r^2) was more than 0.9980. The limits of detection (LODs) and limits of quantitation (LOQs) for BTEX were observed to be 0.002–0.005 μg L^{-1} and 0.008–0.017 μg L^{-1}, respectively. The intra- and inter-batch relative standard deviations (RSDs) were less than 11.6% and 15.0%, respectively.

Received 14th July 2017
Accepted 22nd August 2017

DOI: 10.1039/c7ra07733e

rsc.li/rsc-advances

1 Introduction

Benzene, toluene, ethylbenzene and *o*-, *m*- and *p*-xylene (BTEX) are widely used in the chemical industry and its related fields. As we know, these compounds can cause adverse health effects, such as cancer, liver damage and central nervous system disease.[1] In response to this problem, the WHO drinking water guidelines has established the permissible levels for BTEX (benzene of 10 μg L^{-1}, toluene of 700 μg L^{-1}, ethylbenzene of 300 μg L^{-1} and xylenes of 500 μg L^{-1}) in drinking water.[2] The normalized quality limit for drinking water according to the EPA is 5 μg L^{-1} for benzene, 1000 μg L^{-1} for toluene, 700 μg L^{-1} for ethylbenzene and 10 000 μg L^{-1} for xylenes, respectively.[3] Therefore, establishing a sensitive, reliable, convenient and fast analytical technique to determine BTEX in the environment is urgently required.

Sample preparation is a crucial step for systematic analytical techniques. However, this step is also a significant bottleneck for obtaining an accurate result in an analysis. Several disadvantages of traditional methods of liquid–liquid extraction (LLE) are the use of significant volumes of toxic organic solvents, being time-consuming and causing difficulty in automation. Sorbent-based extraction methods, such as solid phase extraction (SPE) and solid phase microextraction (SPME), use little to no toxic solvents and are the widely used sample preparation methods.[4–6] However, SPE and SPME have some disadvantages such as expense, tediousness and limited lifetime. Recently, magnetic solid phase extraction (MSPE), a sorbent-based extraction technique, has been developed to overcome these limitations.[7] In MSPE, a magnetic sorbent is dispersed into a sample solution where the target analytes are adsorbed onto the sorbent and then separated rapidly and effectively from the solution using an external magnet. Finally, the analytes on the sorbent are eluted using a small amount of organic solvent. The virtues of MSPE, such as magnetic operational simplicity, rapid separation times, analyte retrievability and high extraction efficiency, have allowed it to be successfully used for the determination of different analytes, such as drugs,[8,9] insecticides,[10] phthalic acid esters (PAEs),[11] polycyclic aromatic hydrocarbons (PAHs),[12,13] and metal ions.[14]

[a]*School of Chemistry and Environmental, Fujian Province University Key Laboratory of Analytical Science, Minnan Normal University, Zhangzhou 363000, China. E-mail: maoshengzhang@mnnu.edu.cn; Fax: +86-925-2520035; Tel: +86-925-2591445*
[b]*Dongshan Environmental Protection Bureau, Zhangzhou 363400, China*

For MSPE, the first issue to resolve is the choice of magnetic material. Fe_3O_4 MNPs are mainly used as a magnetic material to prepare the magnetic sorbents due to ease of their synthesis and high magnetic characteristics. For one thing, Fe_3O_4 MNPs can be divided into spherical structure and octahedral structure. According to our knowledge, nearly all the previous research of MSPE has used spherical structured Fe_3O_4 MNPs as magnetic material. On the other hand, pure Fe_3O_4 MNPs show the poor adsorption performance to analytes in MSPE. To overcome the limitation, Fe_3O_4 MNPs coated with functional polymers have attracted tremendous interest both theoretically and experimentally. Currently, many studies have modified the surface of Fe_3O_4 MNPs using silica materials,[15] carbon materials,[16] polydopamine,[17] ionic liquids,[18] polypyrrole[10] and molecular imprinted polymers[19] depending on the physical coating desired or the presence of covalent binding.

Due to the sorptive enrichment of organic analytes, polydimethylsiloxane (PDMS) has been utilized as the adsorbing material in many analytical techniques, such as SPME and stir bar sorptive extraction (SBSE). Previous studies demonstrated that PDMS has excellent adsorption characteristics for nonpolar compounds, such as BTEX,[20] PAHs,[21] pesticides[22] and pharmaceuticals.[23] More importantly, PDMS appears to be highly suited for sampling in complex matrices, since the enrichment is based on the partitioning of analytes into and their dissolution within the polymer. Correspondingly, PDMS has been applied to increasingly complex matrices including foods,[24] soils[25] and biological samples.[26]

For the first time, novel octahedral structured Fe_3O_4@SiO_2@PDMS MNPs have been successfully synthesized. First, Fe_3O_4@SiO_2 MNPs were obtained by forming a thin amorphous silica layer on the octahedral structured Fe_3O_4 MNPs. Second, PDMS was coated onto the surface of the Fe_3O_4@SiO_2 MNPs by a sol–gel process. There are two advantages to this design. The Fe_3O_4@SiO_2@PDMS MNPs effectively combines the powerful magnetic properties of octahedral structured Fe_3O_4 MNPs with the high adsorptivity of the PDMS coating, which facilitates the separation and preconcentration of BTEX from environmental water samples. Additionally, the introduction of the SiO_2 coating onto the Fe_3O_4 MNPs provides a silica-like surface for the Fe_3O_4 that made surface modification with organic silane molecules, such as PDMS, easier. The Fe_3O_4@SiO_2@PDMS MNPs were used as a sorbent for MSPE coupled with gas chromatography-flame ionization detector (GC-FID) for the enrichment and analysis of BTEX in water samples. The experimental parameters affecting the MSPE were studied and optimized. Finally, the applicability of the proposed method to determine BTEX at trace levels in real water samples was evaluated.

2 Experimental

2.1 Chemicals and reagents

Standards containing benzene, toluene, ethylbenzene and xylenes (purity ≥ 99%) were purchased from the Institute for Reference Materials of SEPA (Beijing, China). A mixed stock standard solution of BTEX was prepared with a concentration of 1.00 mg L^{-1} in acetone (LC grade) from Sigma-Aldrich (Steinheim, Germany) and stored in the dark at 4 °C. Aqueous working solutions were prepared daily in ultrapure water (resistivity of 18.2 MΩ cm at 25 °C). The ultrapure water was purified with a Milli-Q water purification system (Millipore Corporation, Billerica, MA, USA). Fe_3O_4 MNPs (diam. 50–100 nm) were purchased from Jingkang Co., Ltd. (Changsha, China). Tetraethyl orthosilicate (TEOS) was purchased from Xilong Chemical Co., Ltd (Shantou, China). Methyltrimethoxysilane (MTMOS) and hydroxy silicone oil (HSO) were purchased from Guobang Chemical Co., Ltd (Jinan, China). Trifluoroacetic acid (TFA) was purchased from Aldrich (Allentown, PA, USA).

2.2 Instruments

A Shimadzu GC-14C gas chromatograph (Shimadzu, Tokyo, Japan) equipped with a split–splitless injector and flame ionization detector (FID) was used for BTEX Analyses. An Rtx-50 fused-silica column (50% phenyl and 50% methyl polysiloxane) 30 m long, 0.25 mm internal diameter, 0.25 μm film thickness (Restek, USA) was used. High purity nitrogen (purity ≥ 99.999%) was employed as the carrier gas at a flow rate of 1.0 mL min^{-1}. The injector temperature was set at 200 °C. The GC oven temperature was initially held at 40 °C for 1 min and then programmed to increase to 80 °C at 5 °C min^{-1} and held for 3 min. The detector temperature was maintained at 250 °C. Hydrogen and air were used as the detector gases at 48 and 450 mL min^{-1}, respectively. The injection volume was 1 μL in the split mode (split ratio 1 : 10). Clarity Shimadzu Chemstation was utilized to control the system and to acquire the analytical data. Under these conditions, the three xylene isomers were separated into two peaks, one contained a mixture of *m*- and *p*-xylene, and the other contained *o*-xylene. For quantification, we combined the integrated the area of the two peaks to calculate the overall concentration of xylenes.

The morphologies of the materials were observed by scanning electron microscopy (SEM) using a Hitachi S4800 (Tokyo, Japan) and transmission electron microscopy (TEM) using a Tecnai G20 (FEI, American). The crystalline structures of the materials were determined by powder X-ray diffraction (XRD, Rigaku Ultima IV) using a Cu Kα radiation ($\lambda = 1.5418$ Å) with 2θ ranging from 5° to 80° with a scan rate of 0.02° per second. The Fourier transform infrared (FTIR) spectra were obtained using a Nicolet iS 10 infrared spectrometer. Magnetic properties were analyzed using an SQUID-VSM (American) at room temperature under an ambient atmosphere.

2.3 Preparation of Fe_3O_4@SiO_2@PDMS MNPs

For the preparation of Fe_3O_4@SiO_2 MNPs, 2 g Fe_3O_4 was dispersed into in 100 mL of isopropanol and sonicated for 10 min at room temperature. Next, 10 mL of TEOS and 60 mL of NH_3H_2O (25%) were added and stirred for 12 h at room temperature under a N_2 atmosphere. The obtained Fe_3O_4@SiO_2 MNPs were separated by an external magnet and washed with water and methanol five times. Finally, the preparation was dried under vacuum at 60 °C for 6 h for further use.

Next, 1 g of the dried Fe_3O_4@SiO_2 MNPs were dispersed in 20 mL of ethanol. Then, 20 mL of MTMOS and 5 mL of HSO

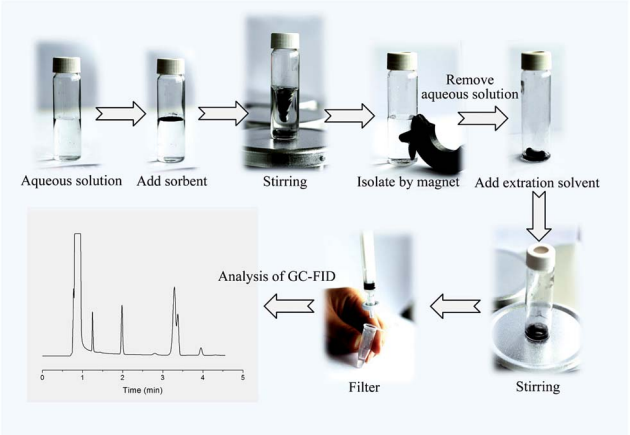

Fig. 1 The schematic representation of proposed MSPE method.

were added and mixed thoroughly by ultrasonic agitation for 20 min. 180 μL of TFA (95%) was sequentially added to the resulting solution with ultrasonic agitation over 3 h. Finally, the product was separated with a magnet, washed repeatedly with water and ethanol, and dried under vacuum at 60 °C.

2.4 MSPE procedure

One hundred milligrams of the Fe_3O_4@SiO_2@PDMS MNPs was added to a 20 mL sample solution containing 5 μg L^{-1} of BTEX. The mixture was continuously stirred at a constant speed (*i.e.*, 200 rpm) with a magnetic stirrer to allow the analytes to be fully adsorbed onto the MNPs. After 15 min, the MNPs were quickly separated from the sample solution using an external magnet. The supernatant was decantated and the MNPs were eluted with 0.5 mL of dichloromethane. The eluting solvent was isolated from MNPs using an external magnet and filtered with a 0.45 μm membrane. Finally, 1.00 μL of the eluting solvent was injected into the GC instrument for subsequent analysis. A schematic representation of the MSPE method is shown in Fig. 1.

3 Results and discussion

3.1 Characterization of the materials

The morphological structure of the Fe_3O_4@SiO_2@PDMS MNPs was characterized with SEM and TEM. The SEM image (Fig. 2a) shows the Fe_3O_4 MNPs have an octahedral structure and uniform size. The estimated average size was 50–100 nm. The TEM image (Fig. 2b) indicates that the bilayer structured SiO_2@PDMS polymerized coatings are homogeneously and uniformly distributed on the surface of the Fe_3O_4 MNPs. The EDX mapping of the Fe_3O_4@SiO_2@PDMS MNPs presented in Fig. 2c contains localized elemental information. This analysis confirms the existence of the elements Si, C, Fe and O in the structure of the Fe_3O_4@SiO_2@PDMS MNPs. Additionally, it shows that the molar ratios of Fe : Si : C are 41 : 5 : 6.

The XRD patterns of the Fe_3O_4, Fe_3O_4@SiO_2 and Fe_3O_4@SiO_2@PDMS MNPs are shown in Fig. 3a. In the pattern from the Fe_3O_4 MNPs, the diffraction angles at 2θ =

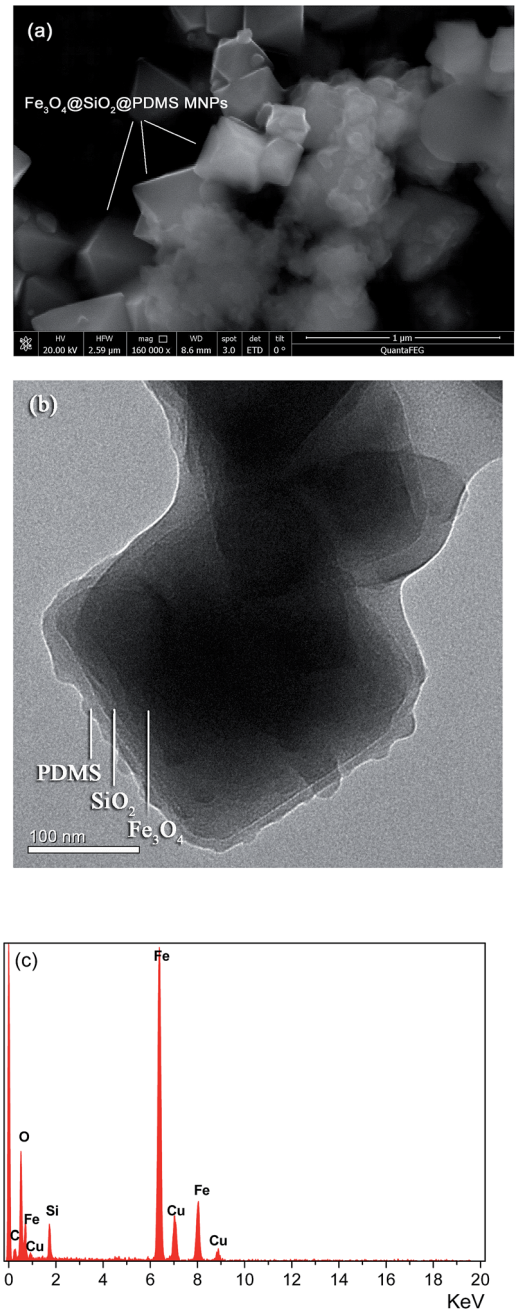

Fig. 2 The SEM image (a), the TEM image (b) and the EDX mapping (c) of the Fe_3O_4@SiO_2@PDMS MNPs.

18.29°, 30.10°, 35.42°, 43.04°, 53.50°, 56.98° and 62.60°, corresponding to the crystal surface of Fe_3O_4 (111), (220), (311), (400), (442), (511) and (440), respectively, confirm the existence of pure Fe_3O_4 (JCPDS 65-3107). The pattern from the Fe_3O_4@SiO_2 MNPs shows almost the same features as the pattern from the Fe_3O_4 MNPs in Fig. 3a. No diffraction peaks corresponding to SiO_2 were observed because the prepared SiO_2 is amorphous. The same set of characteristic peaks were also observed for the Fe_3O_4@SiO_2@PDMS MNPs, indicating the stability of the crystalline phase of the Fe_3O_4 throughout preparation.

Fig. 3b shows the FTIR spectra of the Fe_3O_4, Fe_3O_4@SiO_2 and Fe_3O_4@SiO_2@PDMS MNPs. The stretching vibration modes of Fe–O bands are observed at 573 cm^{-1} in the FTIR spectrum of the Fe_3O_4 MNPs. The characteristic peaks of Si–OH (963 cm^{-1}) and Si–O–Si (1095 cm^{-1}) observed in the spectrum of Fe_3O_4@SiO_2 MNPs suggest that the SiO_2 coating has been successfully distributed onto the surfaces of the Fe_3O_4 MNPs. Compared with the spectra of Fe_3O_4 and Fe_3O_4@SiO_2 MNPs, the spectrum of Fe_3O_4@SiO_2@PDMS MNPs also displays the characteristic peaks of PDMS, including $-CH_3$ at approximately 2900 cm^{-1}, which confirms that the PDMS coating was successfully applied onto the MNPs.

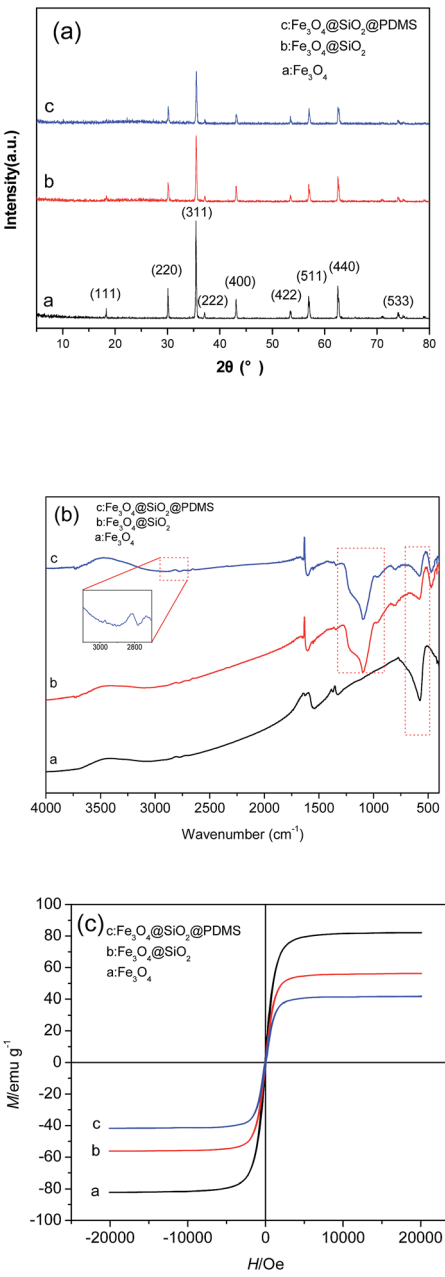

Fig. 3 The XRD patterns (a), the FTIR spectra (b) and the hysteresis loops (c) of the Fe_3O_4, Fe_3O_4@SiO_2 and Fe_3O_4@SiO_2@PDMS MNPs.

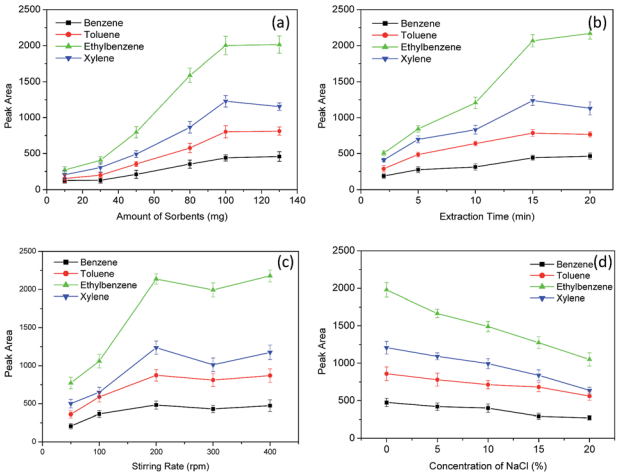

Fig. 4 The effect of amount of the Fe_3O_4@SiO_2@PDMS MNPs (a), extraction time (b), stirring rate (c) and ionic strength (d) on the relative peak area of BTEX.

Fig. 3c shows the hysteresis loops of the Fe_3O_4, Fe_3O_4@SiO_2 and Fe_3O_4@SiO_2@PDMS MNPs. All of the hysteresis loops for the MNPs show an "S" shape and are almost absent of residual magnetism and coercivity force. The saturation magnetization of the Fe_3O_4, Fe_3O_4@SiO_2 and Fe_3O_4@SiO_2@PDMS MNPs are 82.2 emu g^{-1}, 56.2 emu g^{-1} and 41.8 emu g^{-1}, respectively. These results demonstrate that the magnetization decreases with coating. However, the magnetization is still sufficiently high for the MNPs to be separated by an external magnet. These results demonstrate that the sorbents can easily be separated and recovered by an external magnetic field.

3.2 Optimization of extraction conditions

Several parameters, including the amount of sorbent, extraction time, stirring rate, salt effect, the type of desorption solvent, the volume of desorption solvent and desorption time, were

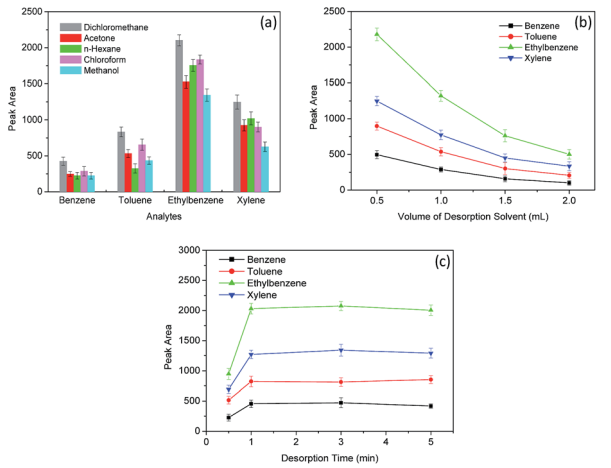

Fig. 5 The effect of type of desorption solvent (a), volume of desorption solvent (b) and desorption time (c) on the relative peak area of BTEX.

Table 1 Linearity range, coefficient of determination (r^2), LODs, LOQs and repeatability of the method

Analytes	Linearity range ($\mu g\ L^{-1}$)	Coefficient of determination (r^2)	LODs ($\mu g\ L^{-1}$)	LOQs ($\mu g\ L^{-1}$)	Repeatability (RSD%)	
					Intra-batch	Inter-batch
Benzene	0.05–20	0.9985	0.005	0.017	8.9	13.4
Toluene	0.05–20	0.9991	0.005	0.017	7.5	11.5
Ethylbenzene	0.05–20	0.9993	0.002	0.008	10.2	15.0
Xylenes	0.05–20	0.9980	0.002	0.008	11.6	14.8

investigated to optimize the extraction efficiency of BTEX by the Fe_3O_4@SiO_2@PDMS MNPs. The concentration of BTEX was set at 5 $\mu g\ L^{-1}$. All of the optimization experiments were conducted three times.

3.2.1 Amount of sorbent. The mass transfer of the analytes from the solution to the sorbent strongly depends on the amount of sorbent. The effect of the amount of the Fe_3O_4@SiO_2@PDMS MNPs was studied in the range 10–130 mg. Based on the results shown in Fig. 4a, the peak areas of the BTEX significantly increased when amount of sorbent increased from 10 to 100 mg and reached a maximum at 100 mg. No significant increase of peak areas was observed with additional sorbent. Therefore, 100 mg of sorbent was selected for further optimizations.

3.2.2 Extraction time. It is necessary to provide sufficient contact time for the analytes and sorbents to reach the adsorption equilibrium. The effect of extraction time on the extraction efficiency of the analytes was examined with the results displayed in Fig. 4b. The peak areas of the BTEX increased continuously when increasing the time from 2 to 15 min, and remained constant with additional time. Accordingly, 15 min was selected as the optimal time.

3.2.3 Stirring rate. Stir was applied to facilitate extraction of BTEX on the sorbent. To evaluate the effect of sample stirring rate, the analytes were extracted at different stirring rates (50, 100, 200, 300 and 400 rpm) and the results are displayed in Fig. 4c. The results reveal that the peak areas of BTEX increased as the stirring rate increased from 50 to 200 rpm and then did not observably increase at higher stirring rates. These results indicate that the 200 rpm stirring speed is suitable for this work.

3.2.4 Salt effect. Ionic strength of sample solution plays an important role in determining sensitivity and precision of the method. The influence of ionic strength on the extraction performance of the sorbent was investigated by adding 0–20% (w/v) NaCl to the solution (Fig. 4d). The results show that the presence of salt has a negative effect on the extraction performance. Therefore, further studies were performed without salt.

3.3 Optimization of desorption conditions

3.3.1 Type of desorption solvent. To achieve complete desorption of the analytes from the surfaces of the Fe_3O_4@SiO_2@PDMS MNPs, different solvents (dichloromethane, acetone, *n*-hexane, chloroform and methanol) were tested. The results in Fig. 5a show that dichloromethane gave the greatest peak areas for BTEX. Therefore, dichloromethane was preferred as a desorption solvent for further experiments.

3.3.2 Volume of desorption solvent. Volume of desorption solvent was another important factor required to be optimized. To evaluate the effect of the volume of desorption solvent on the extraction efficiency, the desorption volumes were varied from 0.2 to 2.0 mL. The results in Fig. 5b demonstrate that the greatest peak area of BTEX was achieved with 0.5 mL of the desorption solvent. Thus, 0.5 mL was selected as the most appropriate desorption volume.

3.3.3 Desorption time. Desorption time also plays a very important role in the recovery of the analytes from the sorbent. Desorption time was studied from 0.5–5.0 min. Fig. 5c clearly shows that the peak area increased with desorption times from 0.5–1.0 min and then remained nearly constant. For further experiments, a desorption time of 1.0 min was chosen.

3.4 Analytical performance

A series of experiments regarding linearity and limits of detection (LODs), limits of quantitation (LOQs), and reproducibility were performed to validate the proposed MSPE method under optimal conditions. The linear concentration range was determined from plots of the peak areas *versus* the concentration of

Table 2 Determination results of BTEX in real samples ($n = 6$)

Sample analyte	Jiulong River of Zhangzhou			Inner lake in a school			Sewage treatment plant		
	Detected ($\mu g\ L^{-1}$)	Recovery[a] (%)	RSD (%)	Detected ($\mu g\ L^{-1}$)	Recovery (%)	RSD (%)	Detected ($\mu g\ L^{-1}$)	Recovery (%)	RSD (%)
Benzene	ND[b]	102.6	9.4	ND	87.4	11.0	ND	111.5	5.7
Toluene	ND	106.5	8.2	ND	90.6	11.5	0.32	106.7	6.5
Ethylbenzene	ND	93.5	4.0	ND	118.0	6.9	ND	89.0	6.7
Xylenes	ND	107.8	3.5	ND	100.4	10.5	ND	101.5	8.5

[a] Recoveries determined at spiked levels of 5 $\mu g\ L^{-1}$. [b] Not detected.

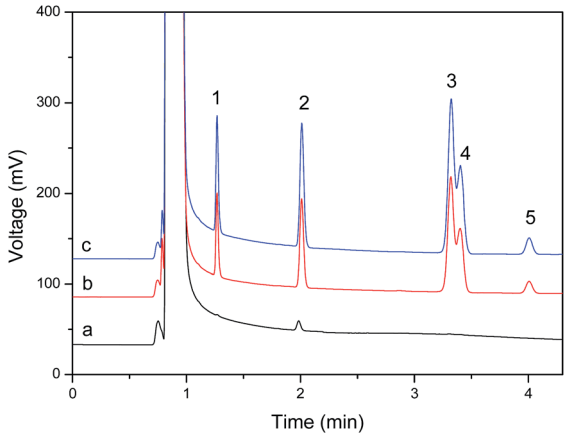

Fig. 6 The representative chromatograms of (a) sewage treatment plant water sample, (b) its corresponding spiked solution with 5 μg L^{-1} BTEX and (c) 5 μg L^{-1} of BTEX standard solution. Peaks: (1) benzene; (2) toluene; (3) ethylbenzene; (4) *m*-, *p*-xylene; (5) *o*-xylene.

the respective analytes. These plots were for quantitative purposes. The LODs and LOQs were calculated at concentrations where the signal-to-noise ratios were equal to 3 and 10. All of the results are summarized in Table 1. Good linearity occurred from 0.05–20 μg L^{-1} and the coefficient of determination (r^2) was more than 0.9980. The LODs and LOQs for BTEX were found to be 0.002–0.005 μg L^{-1} and 0.008–0.017 μg L^{-1}, respectively. To determine the reproducibility of the method, six parallel experiments in quintuple of 5 μg L^{-1} of BTEX with separate intra- and inter-batch preparations were performed. The results show that the intra- and inter-batch relative standard deviations (RSDs) are less than 11.6% and 15.0%, respectively, revealing acceptable reproducibility.

3.5 Analysis of real samples

The developed method was applied to the analysis of BTEX in environmental water samples. Water samples were collected from the Jiulong River of Zhangzhou City, the inner lake of a school and a sewage treatment plant, filtered through 0.45 μm microporous membranes and stored at 4 °C. All samples were analyzed within 3 days of collection to avoid storage losses. The results in Table 2 show that a trace level of toluene (0.32 μg L^{-1}) was detected in the sewage treatment plant water sample. The recovery of the 5 μg L^{-1} of BTEX added to the water samples ranged from 87.4 to 111.5% demonstrating that the accuracy of the suggested method is acceptable. A representative chromatogram of the sewage treatment plant water sample is shown in Fig. 6.

4 Conclusions

In this paper, a new MSPE procedure using Fe_3O_4@SiO_2@PDMS MNPs as sorbents was developed for the determination of BTEX in environmental water samples. The prepared Fe_3O_4@SiO_2@PDMS MNPs have a high surface area, strong magnetic properties, and good adsorption performance for analytes. Under optimal conditions, the proposed MSPE method exhibits high sensitivity, satisfactory recovery in spiked samples and good repeatability for the analysis of BTEX in real water samples.

Conflicts of interest

There are no conflicts to declare.

Acknowledgements

This work was supported by the Natural Scientific Foundation of China (No. 21105088) the Natural Science Foundation of Fujian Province, China (No. 2013J01062) and the Natural Science Foundation of Zhangzhou City, China (No. ZZ2016J30) which are gratefully acknowledged.

References

1 L. M. McKenzie, R. Z. Witter, L. S. Newman and J. L. Adgate, *Sci. Total Environ.*, 2012, **424**, 79–87.
2 WHO, *Drinking Water Guidelines*, 2008.
3 U. S. EPA, *2006 Edition of the Drinking Water Standards and Health Advisories*, 2006.
4 A. Andrade-Eiroa, M. Canle, V. Leroy-Cancellieri and V. Cerdà, *TrAC, Trends Anal. Chem.*, 2015, **80**, 655–667.
5 G. F. Ouyang and J. Pawliszyn, *TrAC, Trends Anal. Chem.*, 2006, **25**, 692–703.
6 M. S. Zhang and J. R. Huang, *RSC Adv.*, 2016, **6**, 94098–94104.
7 T. K. Indira and P. K. Lakshmi, *Int. J. Pharm. Sci. Nanotechnol.*, 2010, **3**, 1035–1042.
8 Y. Y. Sun, J. Tian, L. Wang, H. Y. Yan, F. X. Qiao and X. Q. Qiao, *J. Chromatogr. A*, 2015, **1422**, 53–59.
9 S. Mahpishanian and H. Sereshti, *J. Chromatogr. A*, 2016, **1443**, 43–53.
10 H. Y. Zhao, M. Y. Huang, J. R. Wu, L. Wang and H. He, *J. Chromatogr. B: Anal. Technol. Biomed. Life Sci.*, 2016, **1011**, 33–44.
11 M. Xu, M. H. Liu, M. R. Sun, K. Chen, X. J. Cao and Y. M. Hu, *Talanta*, 2016, **150**, 125–134.
12 H. B. Zheng, J. Ding, S. J. Zheng, G. T. Zhu, B. F. Yuan and Y. Q. Feng, *Talanta*, 2016, **148**, 46–53.
13 Y. T. Shi, H. Wu, C. Q. Wang, X. Z. Guo, J. L. Du and L. M. Du, *Food Chem.*, 2016, **199**, 75–80.
14 B. S. Zhao, M. He, B. B. Chen and B. Hu, *Spectrochim. Acta, Part B*, 2015, **107**, 115–124.
15 L. I. A. Ali, W. A. W. Ibrahim, A. Sulaiman, M. A. Kamboh and M. M. Sanagi, *Talanta*, 2016, **148**, 191–199.
16 C. Herrero-Latorre, J. Barciela-García, S. García-Martín, R. M. Peña-Crecente and J. Otárola-Jiménez, *Anal. Chim. Acta*, 2015, **892**, 10–26.
17 W. B. Chai, H. J. Wang, Y. Zhang and G. S. Ding, *Talanta*, 2016, **149**, 13–20.
18 J. P. Chen and X. S. Zhu, *Food Chem.*, 2016, **200**, 10–15.
19 G. Sheykhaghaei, M. Hossainisadr, S. Khanahmadzadeh, M. Seyedsajadi and A. Alipouramjad, *J. Chromatogr. B: Anal. Technol. Biomed. Life Sci.*, 2016, **1011**, 1–5.

20 N. Baimatova, B. Kenessov, J. A. Koziel, L. Carlsen, M. Bektassov and O. P. Demyanenko, *Talanta*, 2016, **154**, 46–52.
21 W. Lin, S. B. Wei, R. F. Jiang, F. Zhu and G. F. Ouyang, *Anal. Chim. Acta*, 2016, **933**, 117–123.
22 J. Martins, C. Esteves, A. Limpo-Faria, P. Barros, N. Ribeiro, T. Simões, M. Correia and C. Delerue-Matos, *Food Chem.*, 2012, **132**, 630–636.
23 V. K. Balakrishnan, K. A. Terry and J. Toito, *J. Chromatogr. A*, 2006, **1131**, 1–10.
24 A. G. Oomen, P. Mayer and J. Tolls, *Anal. Chem.*, 2000, **72**, 2802–2808.
25 F. Reichenberg, F. Smedes, J. Å. Jönsson and P. Mayer, *Chem. Cent. J.*, 2008, **2**, 1–10.
26 A. Jahnke, P. Mayer, D. Broman and M. S. McLachlan, *Chemosphere*, 2009, **77**, 764–770.